



Ciências
ULisboa

Complementary Astrophysics

L7 - The Interstellar Medium



Ciências
ULisboa

What did we learn?



What did we learn?

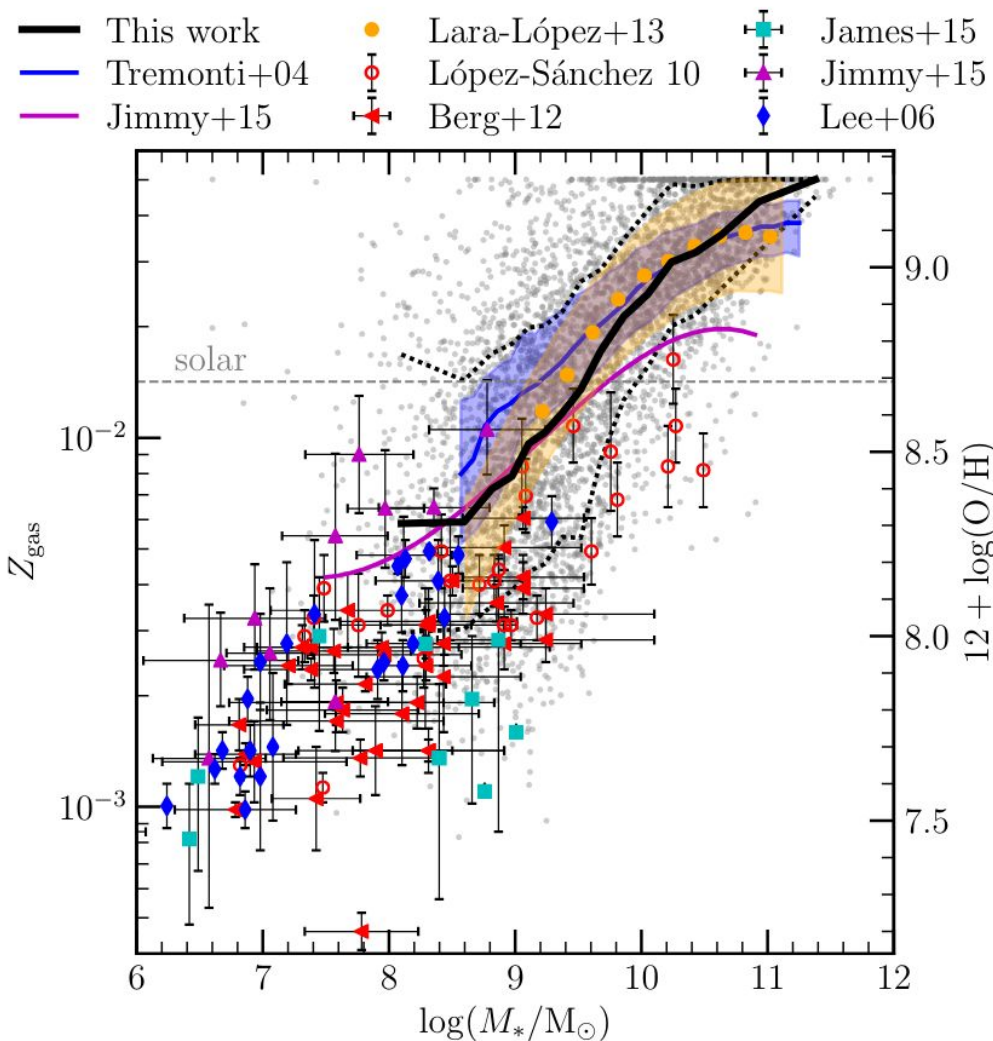
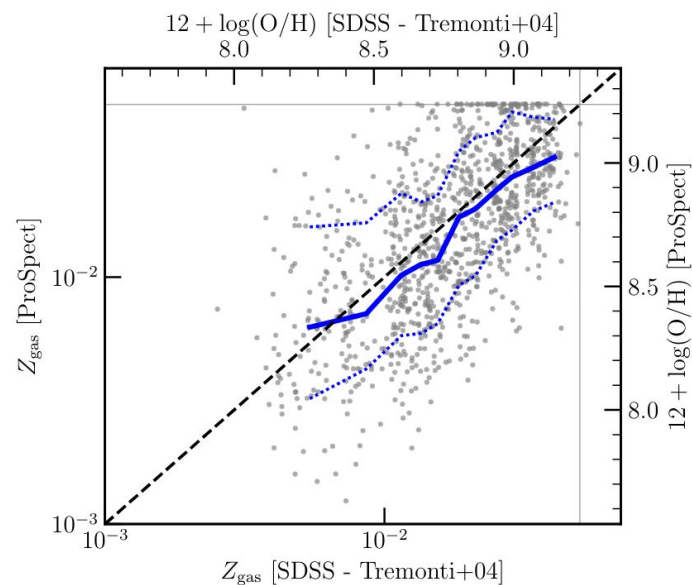
1. Galaxy constituents
2. Star formation cycle
3. Molecular Clouds
4. Star formation Tracer
5. Star Formation Laws
6. Starburst Systems

Galaxy And Mass Assembly (GAMA): The inferred mass–metallicity relation from $z = 0$ to 3.5 via forensic SED fitting

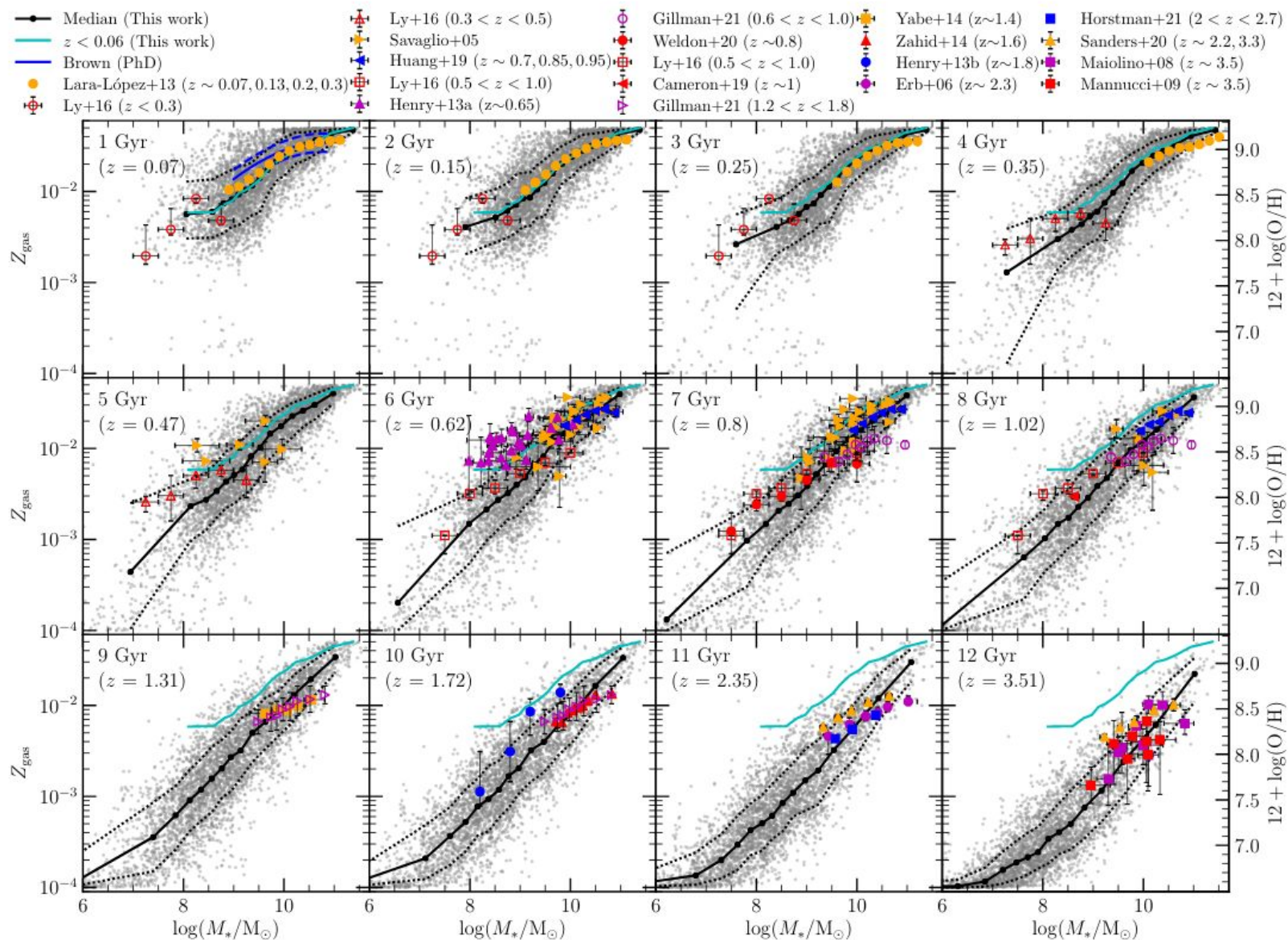
Sabine Bellstedt,^{1*} Aaron S. G. Robotham,^{1,2} Simon P. Driver,¹ Jessica E. Thorne,¹
Luke J. M. Davies,¹ Benne W. Holwerda,³ Andrew M. Hopkins,⁴ Maritza A. Lara-Lopez,⁵
Ángel R. López-Sánchez,^{4,6,2} Steven Phillipps⁷

We analyse the metallicity histories of $\sim 4,500$ galaxies from the GAMA survey at $z < 0.06$ modelled by the SED-fitting code PROSPECT using an evolving metallicity implementation. These metallicity histories, in combination with the associated star formation histories, allow us to analyse the inferred gas-phase mass–metallicity relation. Furthermore, we extract the mass–metallicity relation at a sequence of epochs in cosmic history, to track the evolving mass–metallicity relation with time. Through comparison with observations of gas-phase metallicity over a large range of redshifts, we show that, remarkably, our forensic SED analysis has produced an evolving mass–metallicity relationship that is consistent with observations at all epochs. We additionally analyse the three dimensional mass–metallicity–SFR space, showing that galaxies occupy a clearly defined plane. This plane is shown to be subtly evolving, displaying an increased tilt with time caused by general enrichment, and also the slowing down of star formation with cosmic time. This evolution is most apparent at lookback times greater than 7 Gyr. The trends in metallicity recovered in this work highlight that the evolving metallicity implementation used within the SED fitting code PROSPECT produces reasonable metallicity results over the history of a galaxy. This is expected to provide a significant improvement to the accuracy of the SED fitting outputs.

Highlights



Highlights



Outline of the course

1. History
2. Review of the general concepts
3. Galaxies in our local Universe
4. Galaxies kinematics
5. Scaling relations
6. Star formation
- 7. Interstellar Medium**

ISM: What is?

One of the slides in previous lesson showed that galaxies are essentially ‘void’: the stars are a small fraction of the total volume and the distance between stars is big compared to the galaxy size.

In reality, the interstellar regions are filled with a dilute gas called ISM. The main constituents are:

- 99% = Hydrogen and Helium
- 1% = dust grains and heavy elements

ISM spans ~10 orders of magnitude in density and ~8 order of magnitude in temperature. The number density of the air we breathe is 3×10^{19} atoms/cm³ (extremely diffuse gas but still.....)

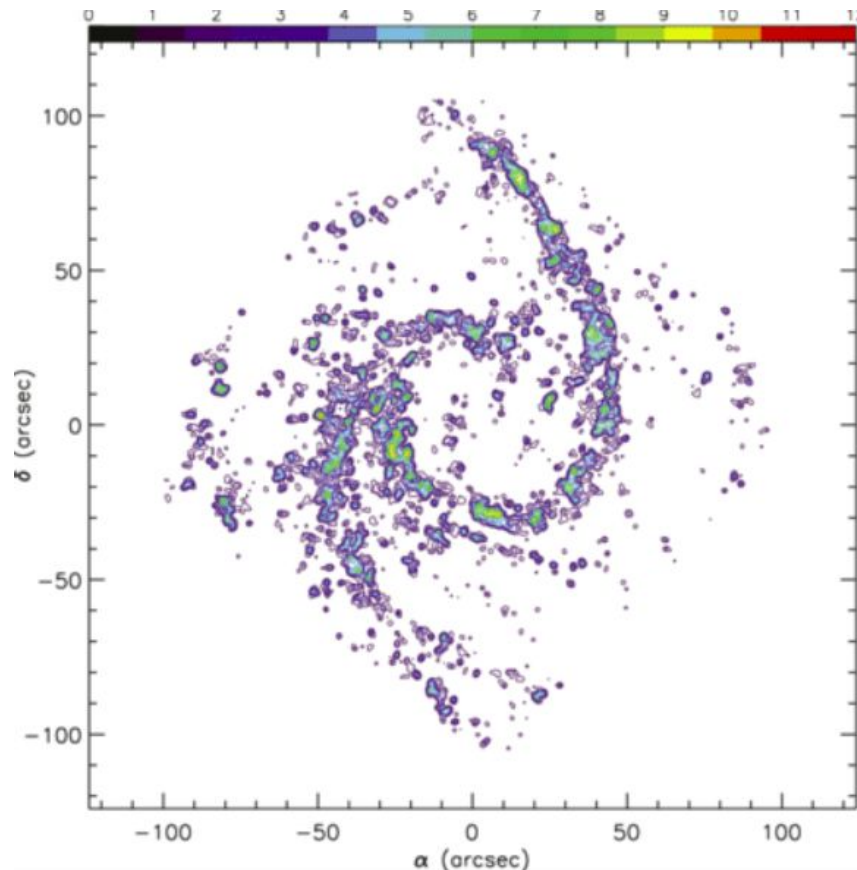
Table 1: Components of the interstellar medium^[3]

Component	Fractional volume	Scale height (pc)	Temperature (K)	Density (particles/cm ³)	State of hydrogen	Primary observational techniques
Molecular clouds	< 1%	80	10-20	10^2 - 10^6	molecular	Radio and infrared molecular emission and absorption lines
Cold neutral medium (CNM)	1-5%	100-300	50-100	20-50	neutral atomic	H I 21 cm line absorption
Warm neutral medium (WNM)	10-20%	300-400	6000-10000	0.2-0.5	neutral atomic	H I 21 cm line emission
Warm ionized medium (WIM)	20-50%	1000	8000	0.2-0.5	ionized	H α emission and pulsar dispersion
H II regions	< 1%	70	8000	10^2 - 10^4	ionized	H α emission and pulsar dispersion
Coronal gas Hot ionized medium (HIM)	30-70%	1000-3000	10^6 - 10^7	10^{-4} - 10^{-2}	ionized (metals also highly ionized)	X-ray emission; absorption lines of highly ionized metals, primarily in the ultraviolet

ISM: What is?

The ISM represents ~10-15% of the total mass of the Galactic disk. The distribution of the ISM is not homogeneous, concentrating near the Galactic plane and along the spiral arms.

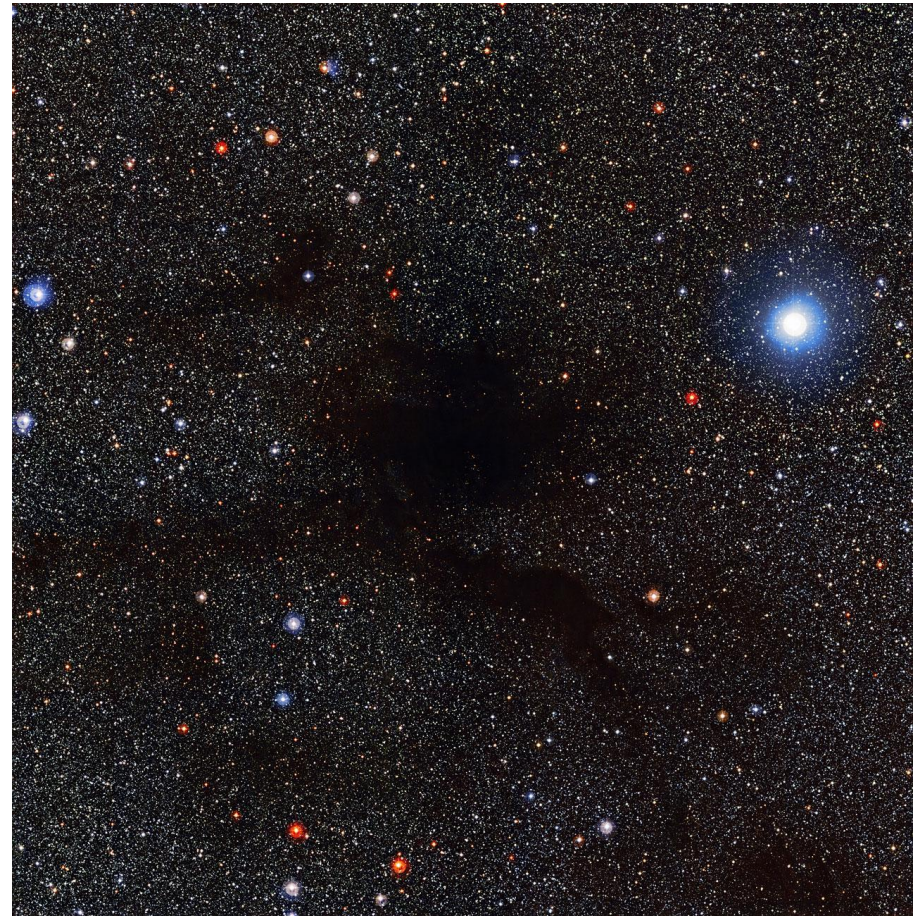
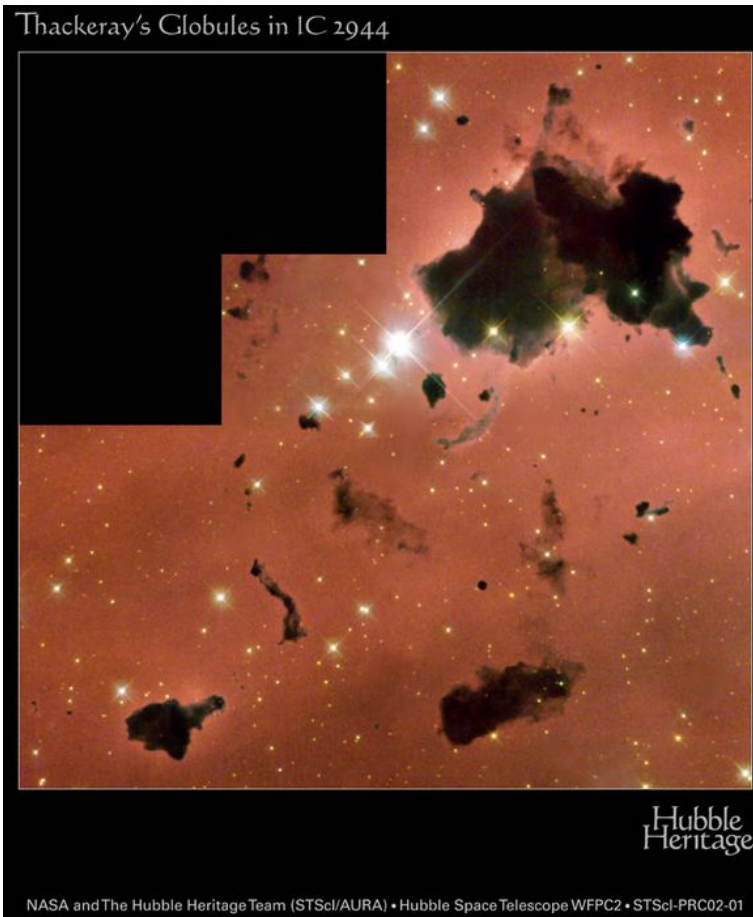
Half of the ISM mass is in discrete clouds occupying ~1-2 % of the interstellar volume.



Type of Clouds

The interstellar clouds can be divided into three types:

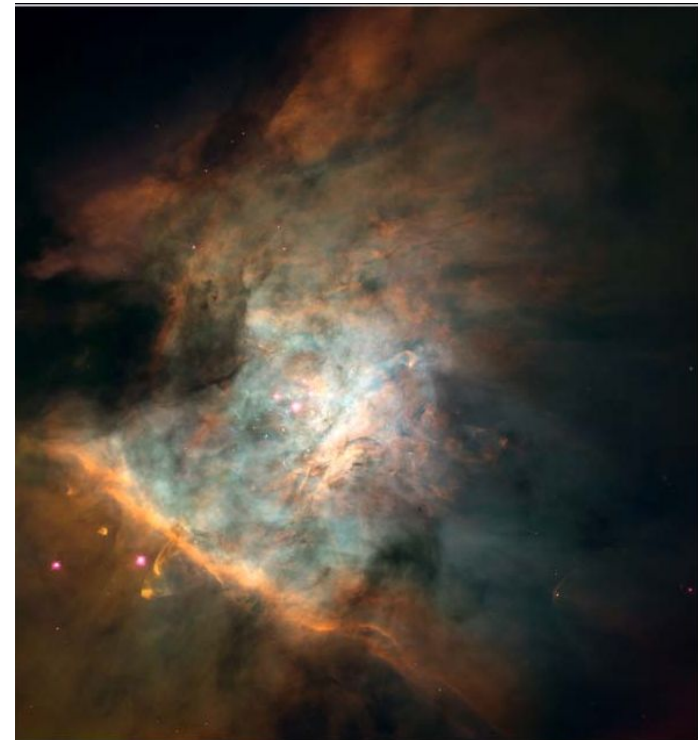
- a) **Dark Clouds:** made of very cold molecular gas ($T \sim 10\text{-}20$ K) that absorbs the light from background stars.



Type of Clouds

The interstellar clouds can be divided into three types:

- b) **Diffuse Clouds:** made of cold atomic gas ($T \sim 100$ K)
almost transparent to the background starlight, except at
specific wavelengths, giving rise to the absorption lines.



Orion Nebula Mosaic

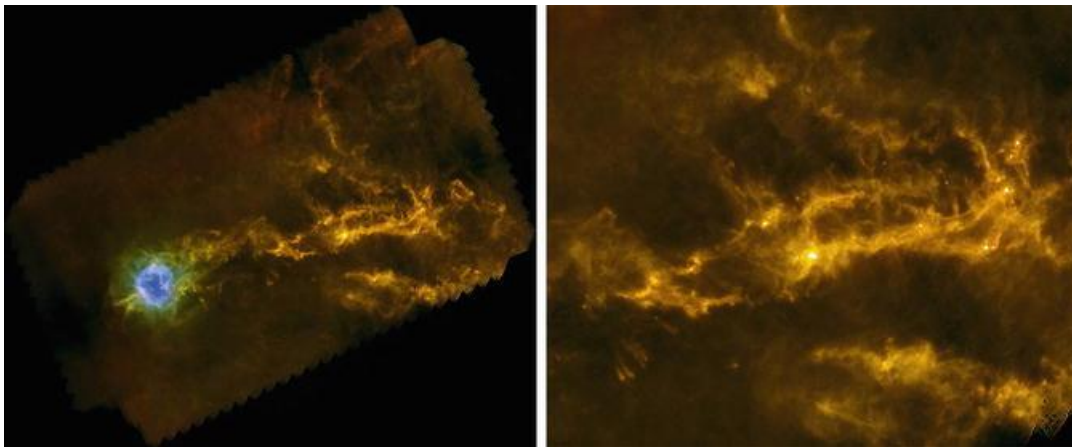
HST · WFPC2

PRC95-45a · ST ScI OPO · November 20, 1995
C. R. O'Dell and S. K. Wong (Rice University), NASA

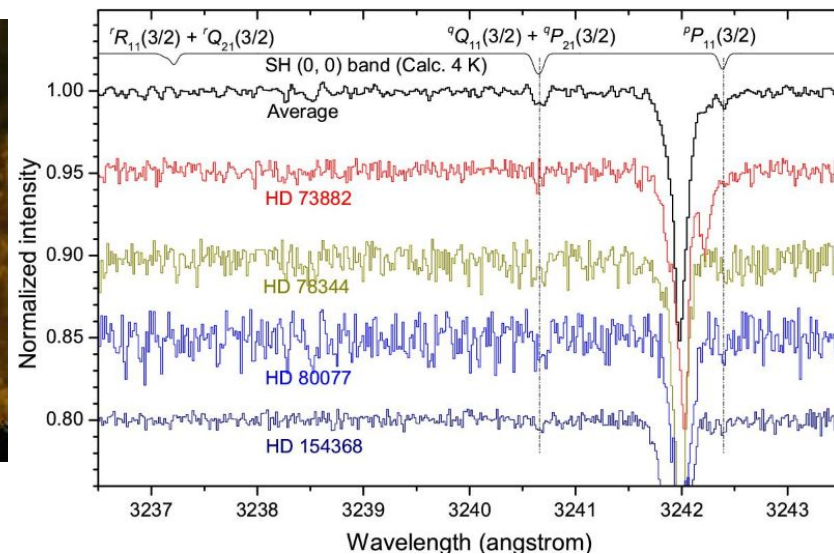
Type of Clouds

The interstellar clouds can be divided into three types:

c) **Translucent Clouds:** made of molecular and atomic gases, shows intermediate visual extinctions.



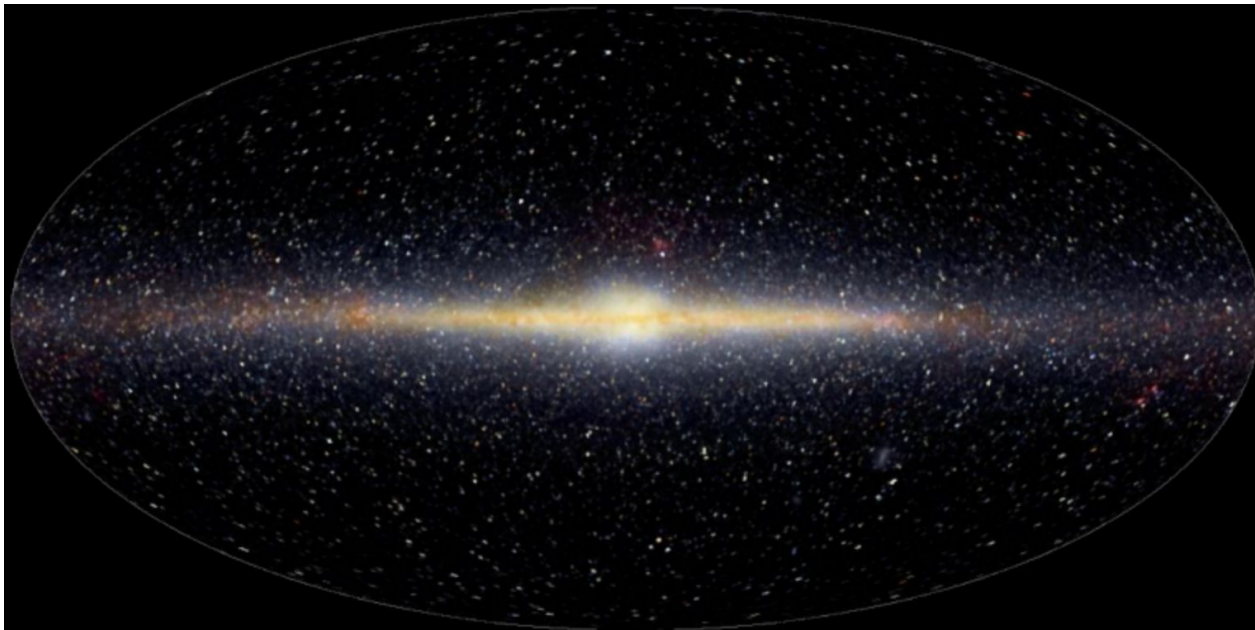
Zhao et al. 2015

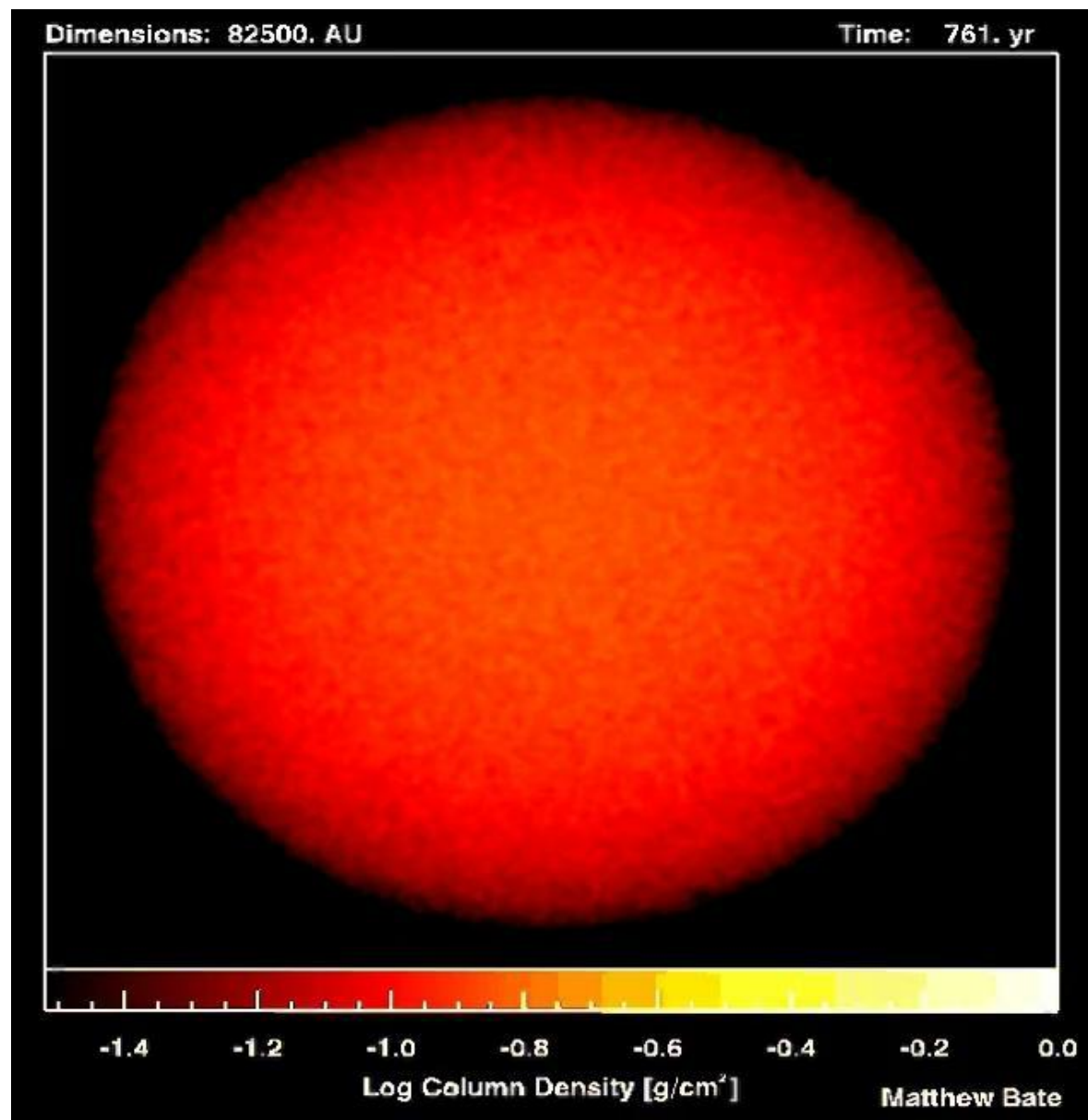


ISM

The interstellar clouds can be divided into three types:

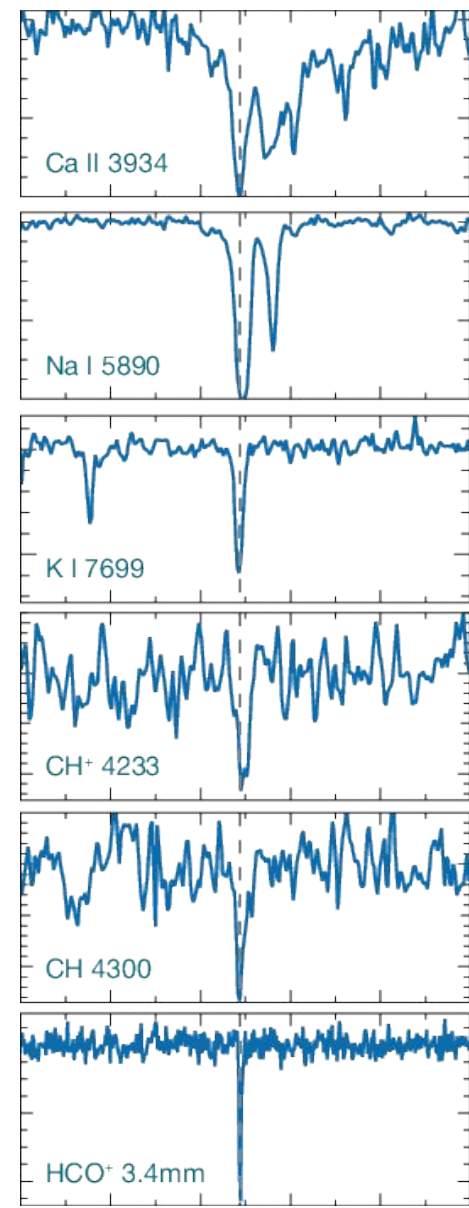
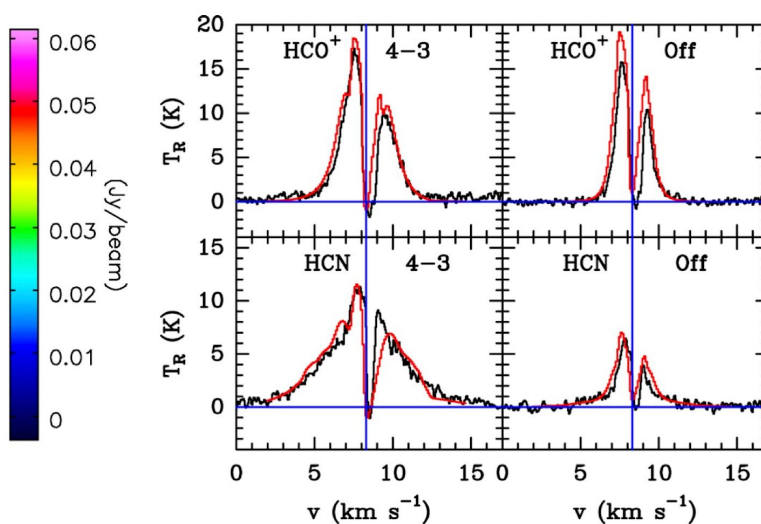
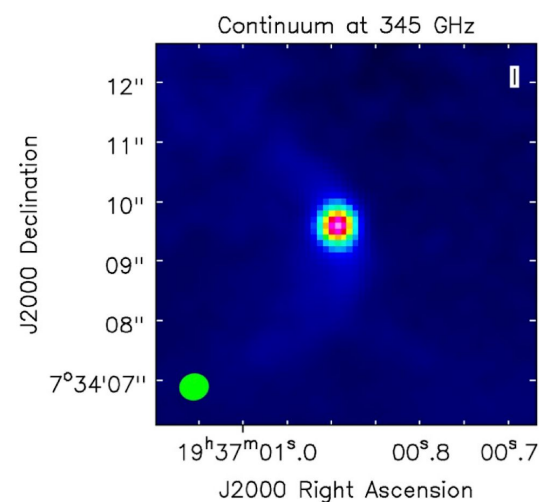
- a) **Dark Clouds:** made of very cold molecular gas ($T \sim 10\text{-}20\text{ K}$) that absorbs the light from background stars
- b) **Diffuse Clouds:** made of cold atomic gas ($T \sim 100\text{ K}$) almost transparent to the background starlight, except at specific wavelengths, giving rise to the absorption lines.
- c) **Translucent Clouds:** made of molecular and atomic gases, shows intermediate visual extinctions.





ISM: Molecular

- Interstellar molecules (CH, CH⁺, and CN) were discovered in the late 1930s, through the analysis of the optical absorption lines in stellar spectra.
- In 1970 ultraviolet astronomy from above the Earth's atmosphere detected the most abundant interstellar molecule, H₂.
- CO, the second most abundant element, was identified in a UV stellar spectrum in Smith and Stecher, 1971.



ISM: Molecular

Molecular gas is structured in discrete clouds:

- giant complexes with sizes of a few tens of parsecs, a mass of $M \sim 10^6 M_{\odot}$, and hydrogen number density $n \sim 100\text{--}1000 \text{ cm}^{-3}$
- small dense cores with sizes of a few tenths of a parsec, a mass $M \sim 0.3\text{--}10^3 M_{\odot}$, and hydrogen number density $\sim 10^4\text{--}10^6 \text{ cm}^{-3}$.

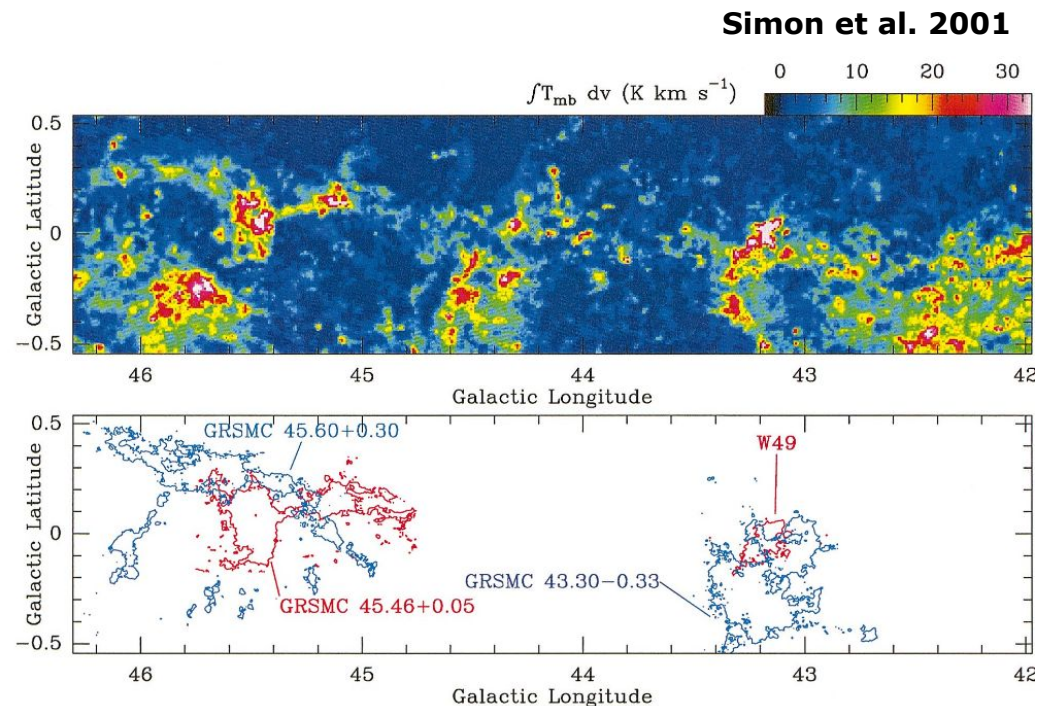
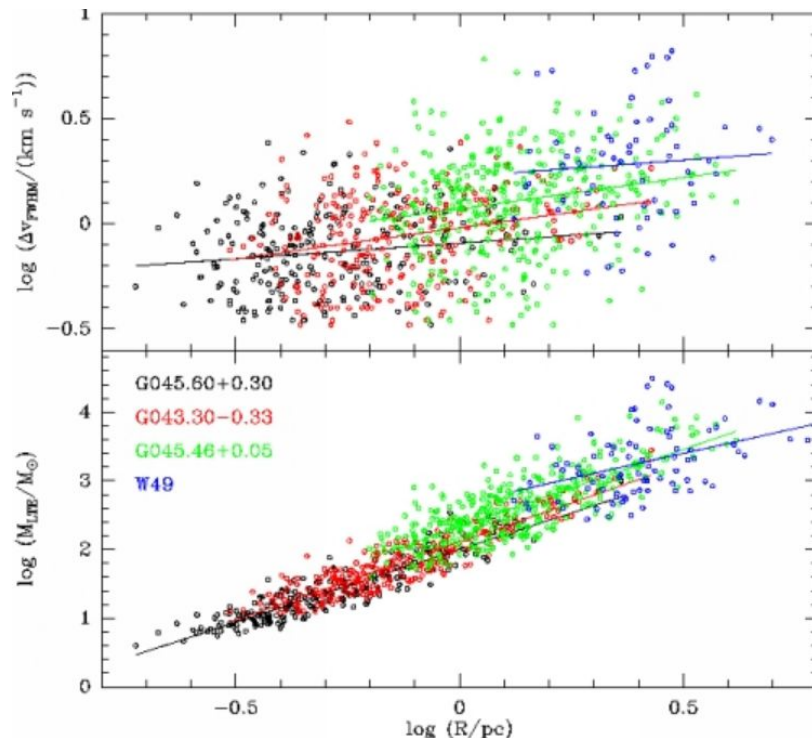


ISM: Molecular

Most of the molecular clouds are sufficiently massive to be in dynamic equilibrium because of self-gravity, satisfying the virial theorem, $G \cdot M/R \sim \sigma^2$, (M , R , and σ are the cloud mass, radius, and internal velocity dispersion, G is the gravitational constant).

Measurements of the CO emission lines show that molecular clouds are very cold, with temperatures around 10-20 K (Goldsmith, 1987).

Thermal speeds at these temperatures are negligible with respect to internal velocity dispersions. This means that the gas pressure inside molecular clouds is dominated by internal turbulent motions.

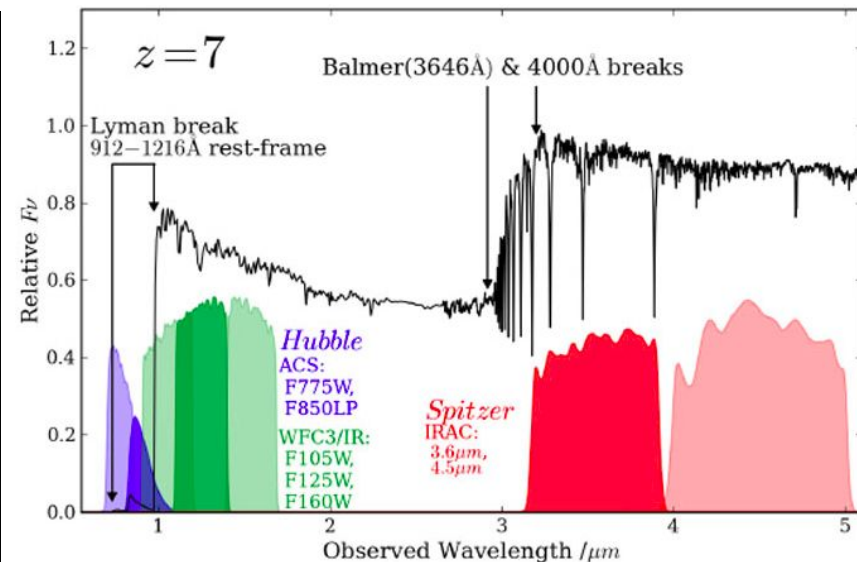
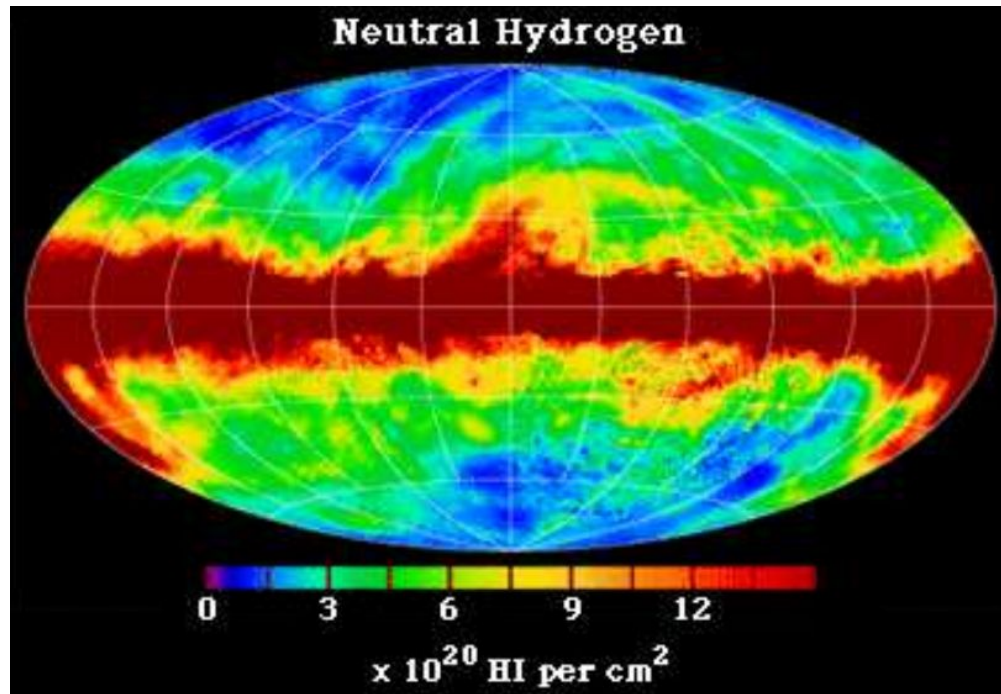


ISM: Neutral

Neutral atomic hydrogen, usually denoted by HI (as opposed to HII for ionized hydrogen), is not observable at optical wavelengths: particle collisions are so rare that nearly all hydrogen atoms have their electron in the ground energy level.

All the electronic transitions between the ground level and an excited state (the Lyman series) fall in the UV regime, with the most common line, Lyman α ($n=2 \rightarrow n=1$) being at 1216 Å.

Dickey & Lockman 1990

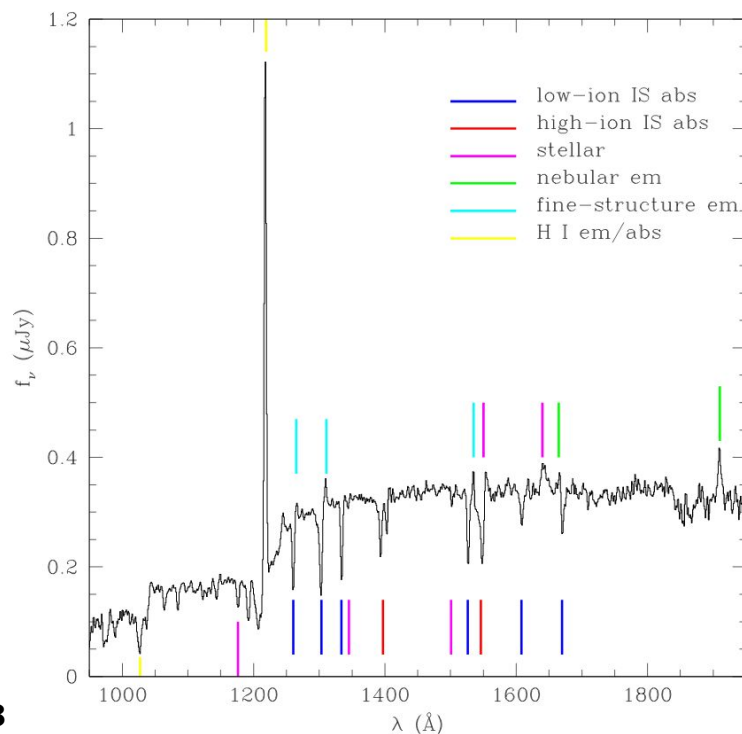


ISM: Neutral

Neutral atomic hydrogen, usually denoted by HI (as opposed to HII for ionized hydrogen), is not observable at optical wavelengths: particle collisions are so rare that nearly all hydrogen atoms have their electron in the ground energy level.

All the electronic transitions between the ground level and an excited state (the Lyman series) fall in the UV regime, with the most common line, Lyman α ($n=2 \rightarrow n=1$) being at 1216 Å.

FIG. 2.— A composite rest-frame UV spectrum constructed from 811 individual LBG spectra. Dominated by the emission from massive O and B stars, the overall shape of the UV continuum is modified shortward of Ly α by a decrement due to inter-galactic HI absorption. Several different sets of UV features are marked: stellar photospheric and wind, interstellar low- and high-ionization absorption, nebular emission from H II regions, Si II* fine-structure emission whose origin is ambiguous, and emission and absorption due to interstellar HI (Ly α and Ly β). There are numerous weak features which are not marked, as well as several features bluewards of Ly α which only become visible by averaging over many sightlines through the IGM. The composite LBG spectrum is available in electronic form from <http://www.astro.caltech.edu/~aes/lbgspec/>.

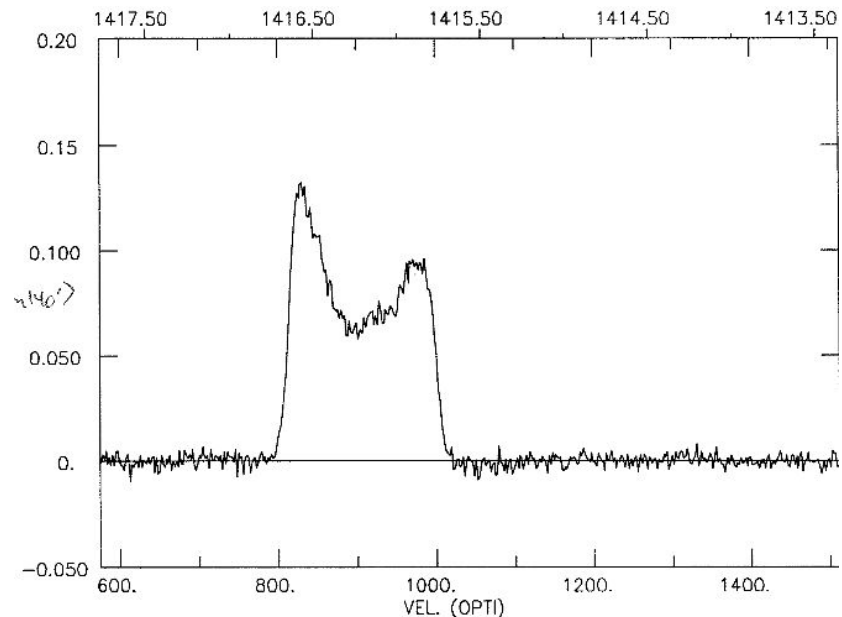
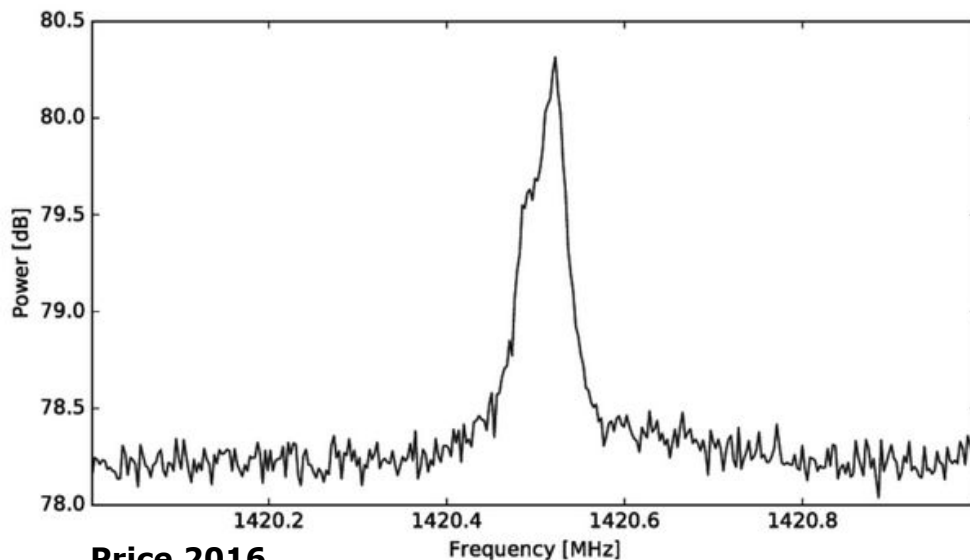


ISM: Neutral

The event that opened the era of radio-astronomical observations of interstellar HI was the detection of the interstellar 21-cm line emission predicted by Hendrik van de Hulst.

This line is due to the “hyperfine” structure of the hydrogen atom: the interaction between the magnetic moment of the electron and that of the proton leads to a splitting of the electronic ground level into two extremely close energy levels, in which the electron spin is either parallel (upper level) or antiparallel (lower level) to the proton spin.

It is the “spin-flip” transition between these two energy levels that correspond to the now-famous 21-cm line. The major advantage of 21-cm photons resides in their ability to penetrate deep into the ISM, thereby offering a unique opportunity to probe the interstellar HI gas out to the confines of the Milky Way.



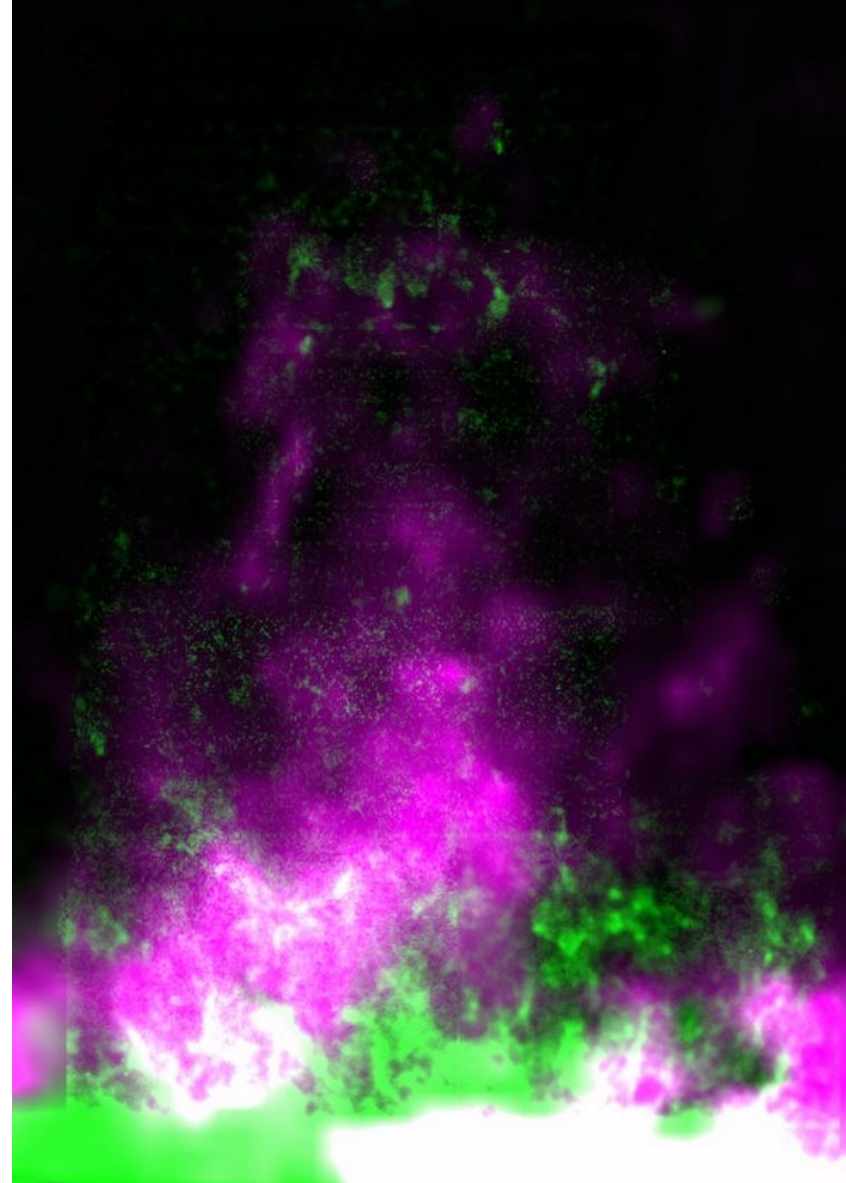
ISM: Neutral

The event that opened the era of radio-astronomical observations of interstellar HI was the detection of the interstellar 21-cm line emission predicted by Hendrik van de Hulst.

This line is due to the “hyperfine” structure of the hydrogen atom: the interaction between the magnetic moment of the electron and that of the proton leads to a splitting of the electronic ground level into two extremely close energy levels, in which the electron spin is either parallel (upper level) or antiparallel (lower level) to the proton spin.

It is the “spin-flip” transition between these two energy levels that correspond to the now-famous 21-cm line. The major advantage of 21-cm photons resides in their ability to penetrate deep into the ISM, thereby offering a unique opportunity to probe the interstellar HI gas out to the confines of the Milky Way.

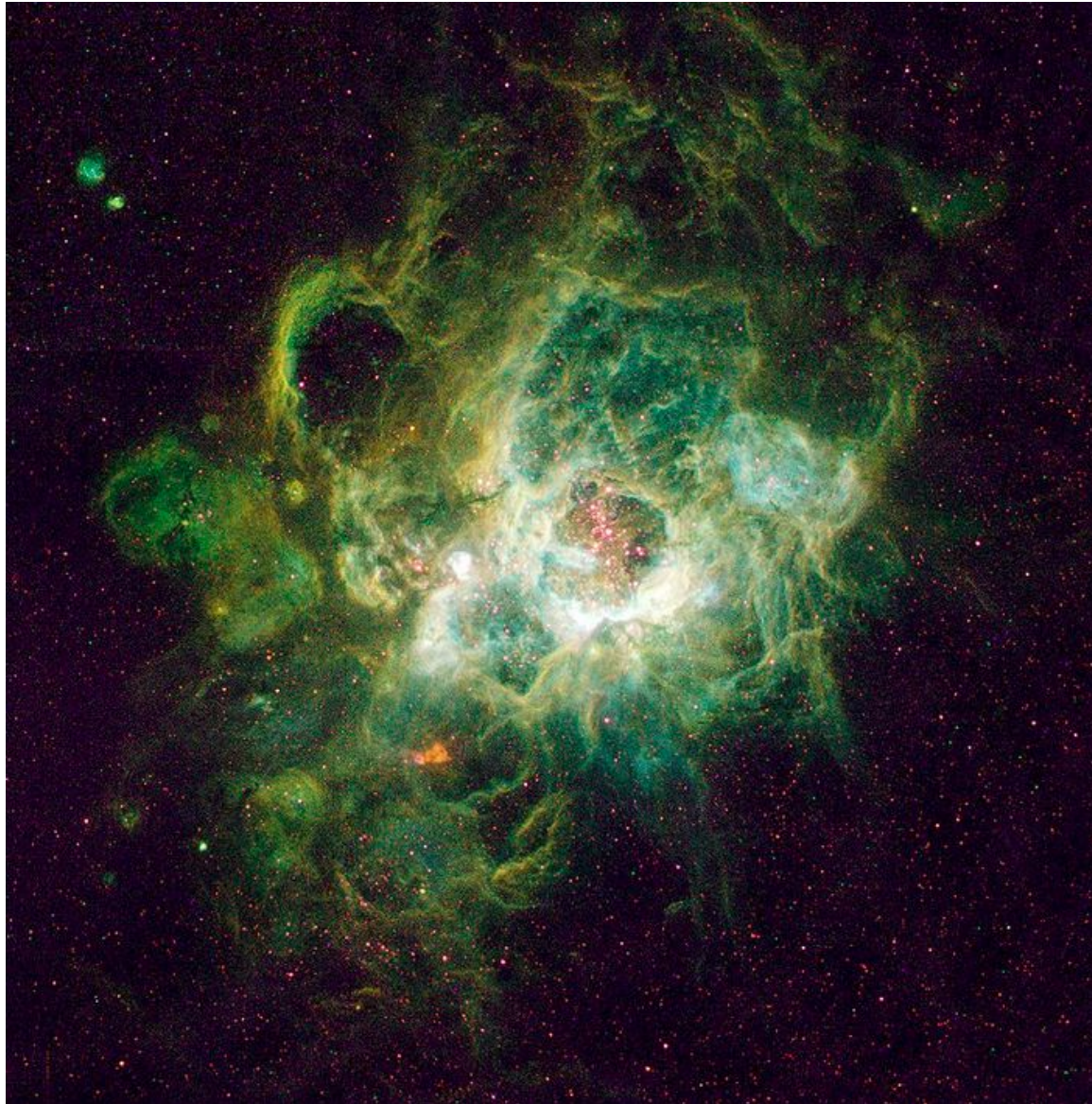
This image shows a galactic "superbubble" in HI (green) and HII (purple) about 7 kpc distant and 3 kpc in height. Stellar winds and supernovae in young star clusters blow these bubbles. Images of HI away from the galactic plane are easily contaminated by sidelobe responses to the strong and widespread HI emission from the plane itself. The low sidelobe levels of the clear-aperture GBT make such HI images possible. Image credit: NRAO



Warm ISM

- O and B stars, massive and hot, emit a strong UV radiation which below 912\AA (corresponding to an energy of 13.6 eV), is sufficiently energetic to ionize hydrogen atoms. For this reason, these stars are surrounded by HII regions within which hydrogen is almost fully ionized.

- Ionizing UV photons are promptly absorbed by neutral hydrogen, and the transition between the HII region and the ambient ISM is abrupt. Inside the HII region, ions and free electrons keep recombining before being separated again by fresh UV photons from the central star. Thus, the HII region grows until the rate of recombinations within it becomes large enough to balance the rate of photoionizations.

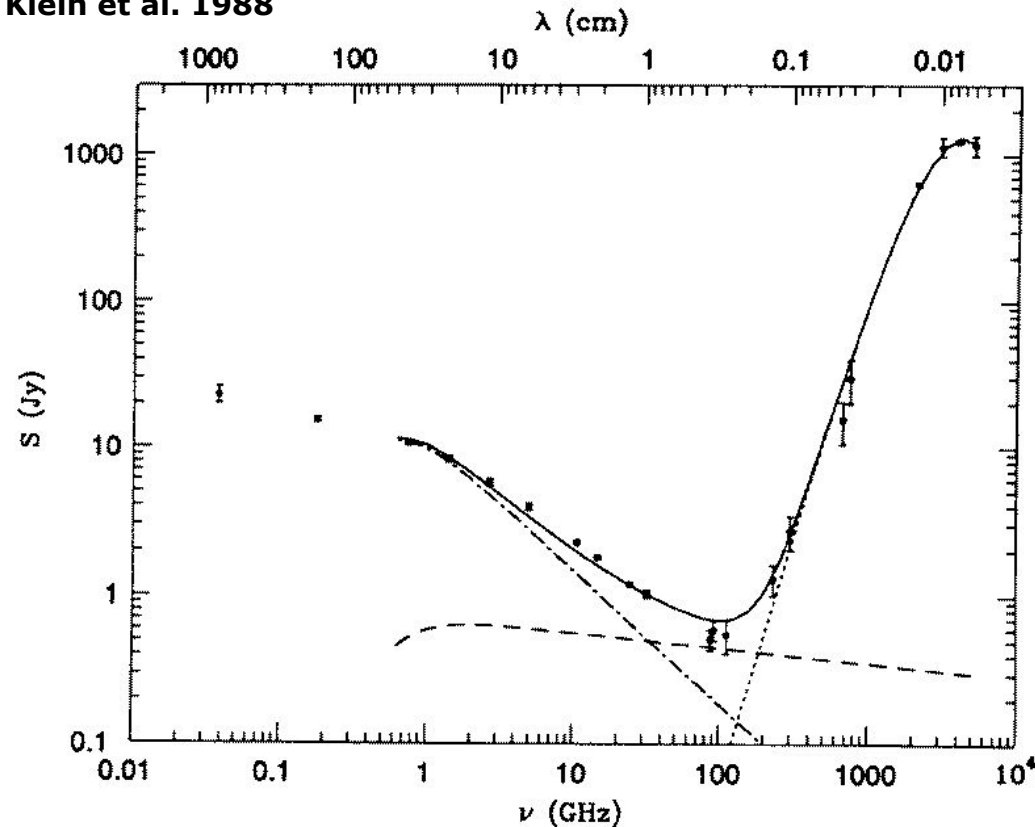


NGC 604, a giant H II region in the Triangulum Galaxy

Warm ISM

The radio continuum radiation of an HII region arises from the “bremsstrahlung” or “free-free” emission generated as free electrons are accelerated in the Coulomb field of positive ions (H^+ , He^+ , He^{++}).

Klein et al. 1988



The observed radio/FIR spectrum of M82 is the sum (solid line) of synchrotron (dot-dash line), free-free (dashed line), and dust (dotted line) components.

Paron et al. 2013

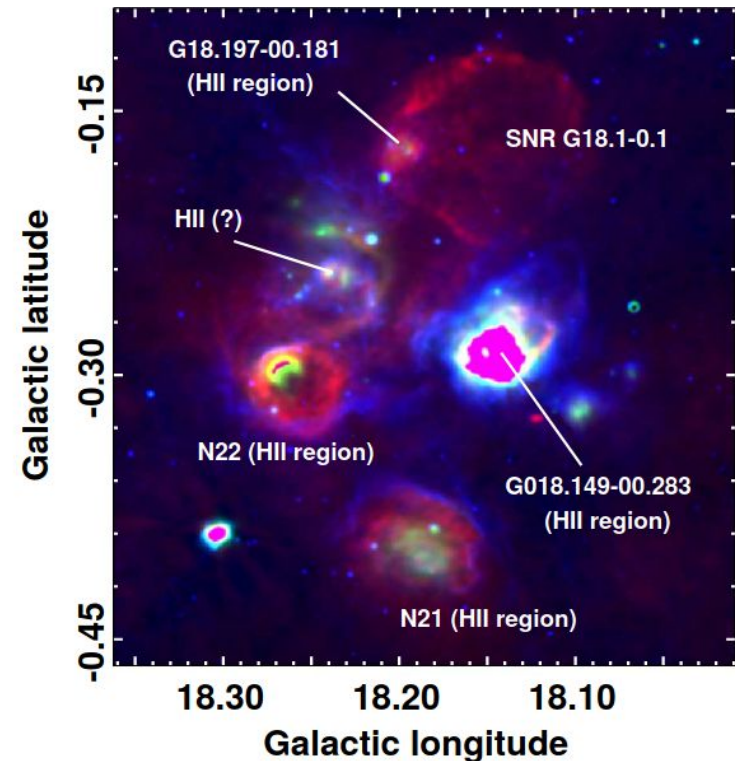
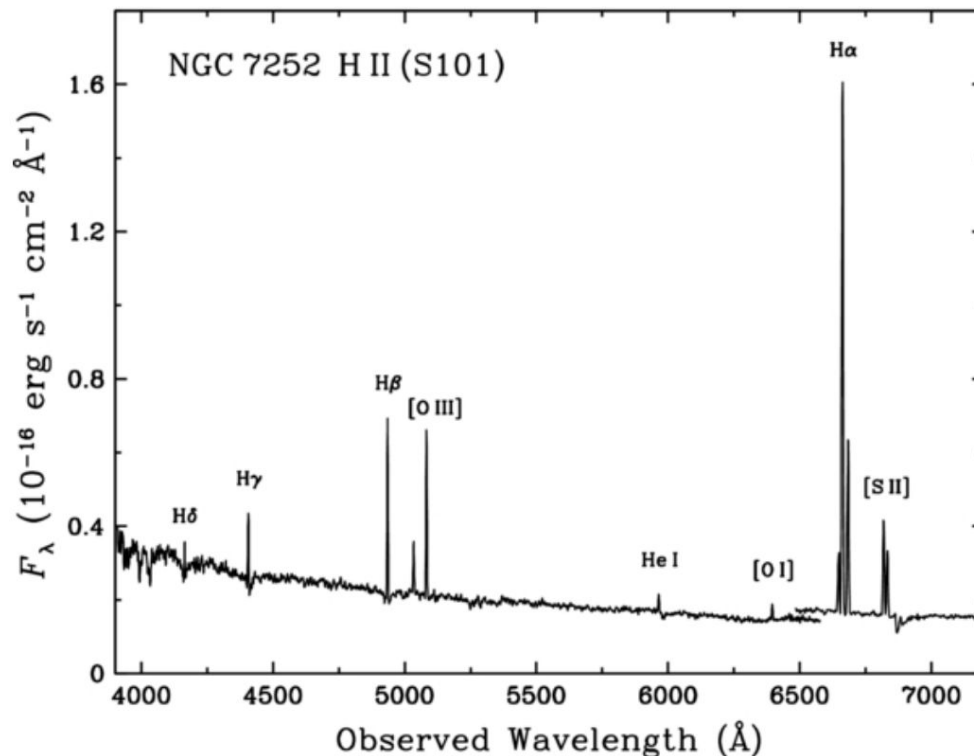


Figure 1. The studied region presented in a three-colour image. The radio continuum emission at 20 cm is displayed in red, the IRAC-*Spitzer* 8 μ m emission in blue and the MIPS-*Spitzer* 24 μ m emission is shown in green. The objects analysed in this work are indicated. The arc feature in N22 and almost the whole interior of G18.149-0.283 are saturated in 24 μ m.

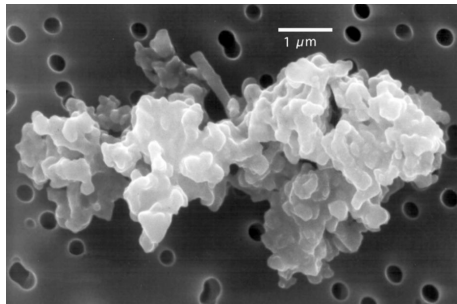
Warm ISM

- Emission lines, found at optical, infrared, and radio wavelengths, are primarily due to radiative recombination of hydrogen and helium ions with free electrons, and to radiative de-excitation of collisionally excited ionized metals.
- Of special importance are the optical hydrogen Balmer lines produced by electronic transitions from an excited state $n > 2$ to the first excited state $n=2$ because each recombination of a free proton with a free electron into an excited hydrogen atom leads sooner or later to the emission of one Balmer photon.

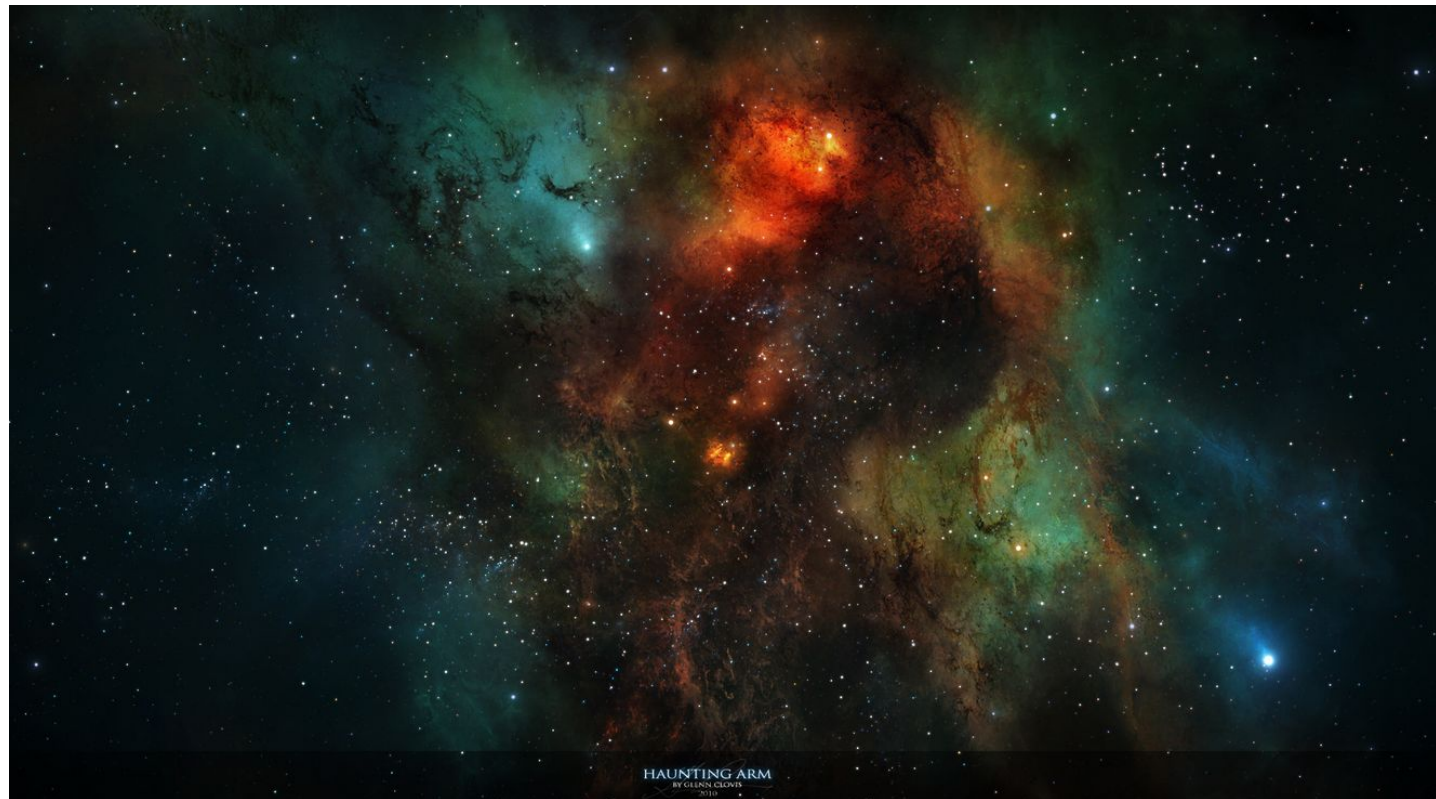


Dust

The dust is made of particles of silicates, carbon, ice, and iron with a typical size of 0.1 microns. Optical and UV emission, at similar wavelengths, can be scattered or absorbed by dust: interstellar reddening.

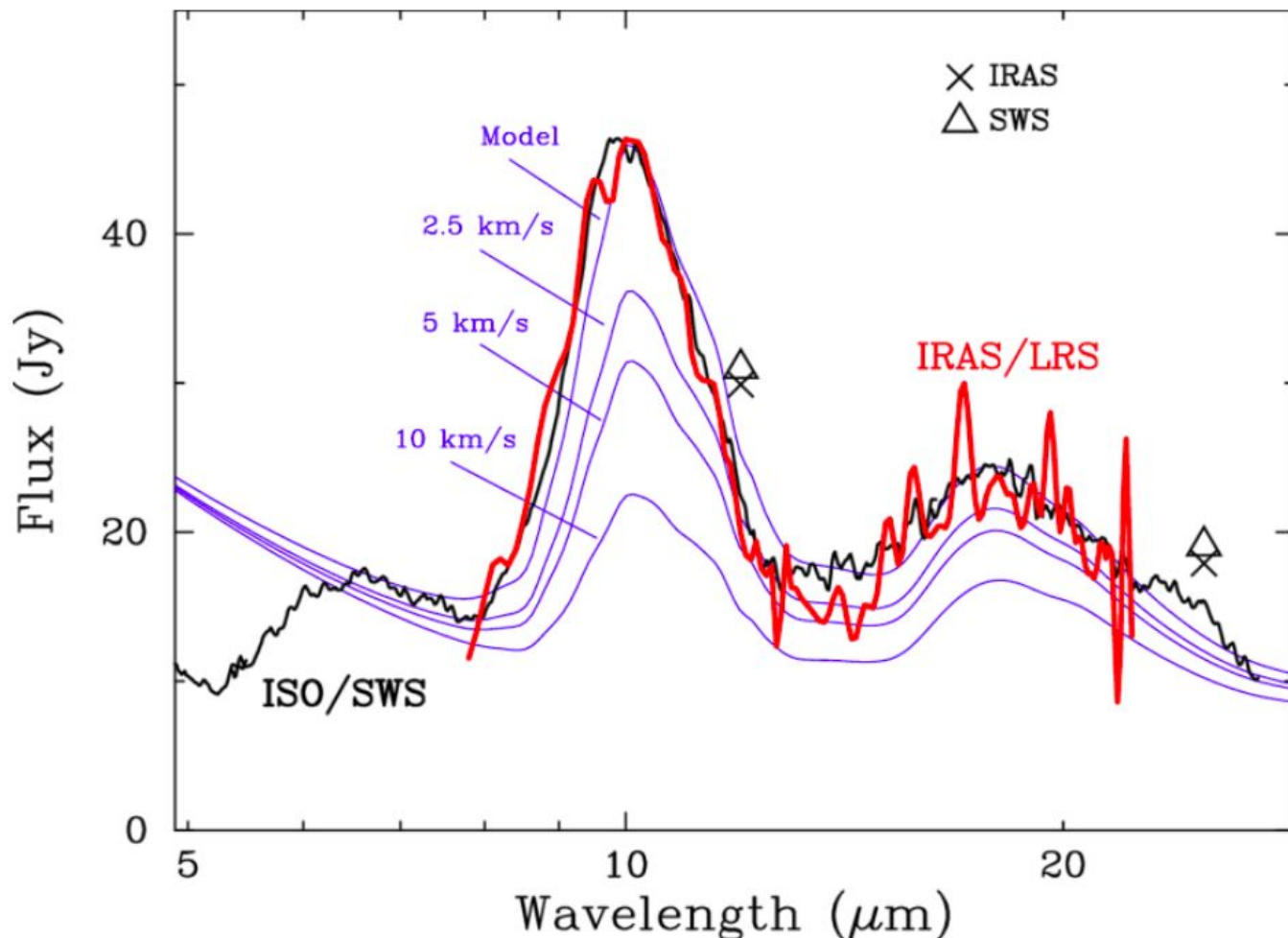


**Porous chondrite
interplanetary dust**



Dust

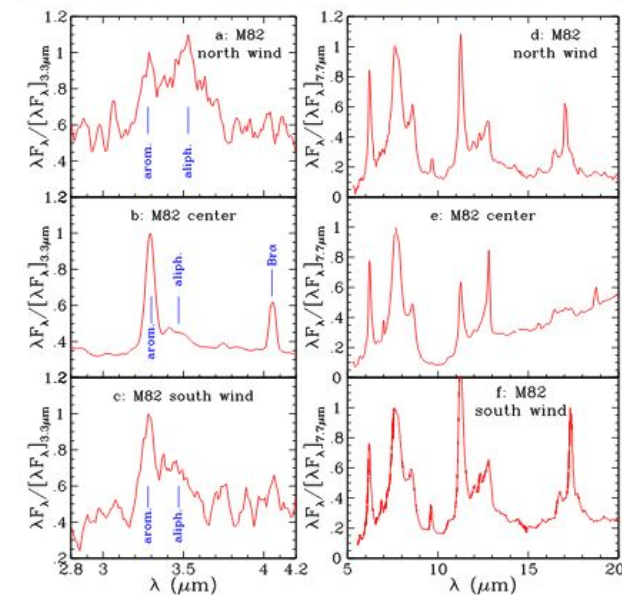
- The dust is made of particles of silicates, carbon, ice, and iron with a typical size of 0.1 microns.
- Optical and UV emission, at similar wavelengths, can be scattered or absorbed by dust: interstellar reddening.
- The IR bands at 9.7 μm and 18 μm maybe imputed to amorphous silicates (Knacke and Thomson, 1973; Draine and Lee, 1984).



The silicate emission bands in the spectra of V778 Cyg observed by the ISO/SWS and the IRAS/LRS. The LRS is scaled on the basis of IRAS 12 μm photometry flux. The agreement between the two spectra is remarkable. The IRAS 12 and 25 μm photometry flux (\times) and corresponding flux measured on the present SWS spectrum (Δ) also agree very well. The thin lines indicate dust model spectra, and the expected change of the dust features during 14 years, assuming that the dust is in a detached shell expanding with velocities as indicated.

- The carrier of a set of five mid-IR emission lines between 3.3 and 11.3 μm has been identified with polycyclic aromatic hydrocarbons (PAHs; Duley and Williams, 1981; Leger and Puget, 1984).
- Other weaker features attest to the presence of additional species, amongst which amorphous carbon and organic refractory material (Tielens and Allamandola, 1987).

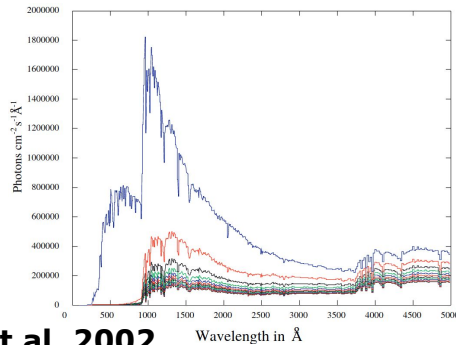
Figure 4: **PAHs in the superwind of M82.** Upper panel: The galaxy is shown as the diffuse bar of blue light. The *Spitzer*/IRAC 8 μm emission, dominated by PAHs, is shown in red. The superwind, emanating from the central starburst region, is evident in the 8 μm emission. The PAH emission is seen all around the galaxy, well beyond the cone defined by the superwind. Lower panel: The near-IR AKARI and mid-IR *Spitzer*/IRS spectra of the north wind (a, d), the center (b, e), and the south wind (c, f) of M82^{88,89}. Most notably, while in the center the 3.3 μm aromatic C–H band is much stronger than the 3.4 μm aliphatic C–H band (b), in the wind the aliphatic band is so pronounced that it even dwarfs the aromatic band (a, c). The intensities of the 11.3, 12.7 and 17.1 μm bands relative to the 6–9 μm bands are stronger in the wind (d, f) than in the center (f). The *Spitzer*/IRAC 8 μm image is adapted from ref.⁸⁷.



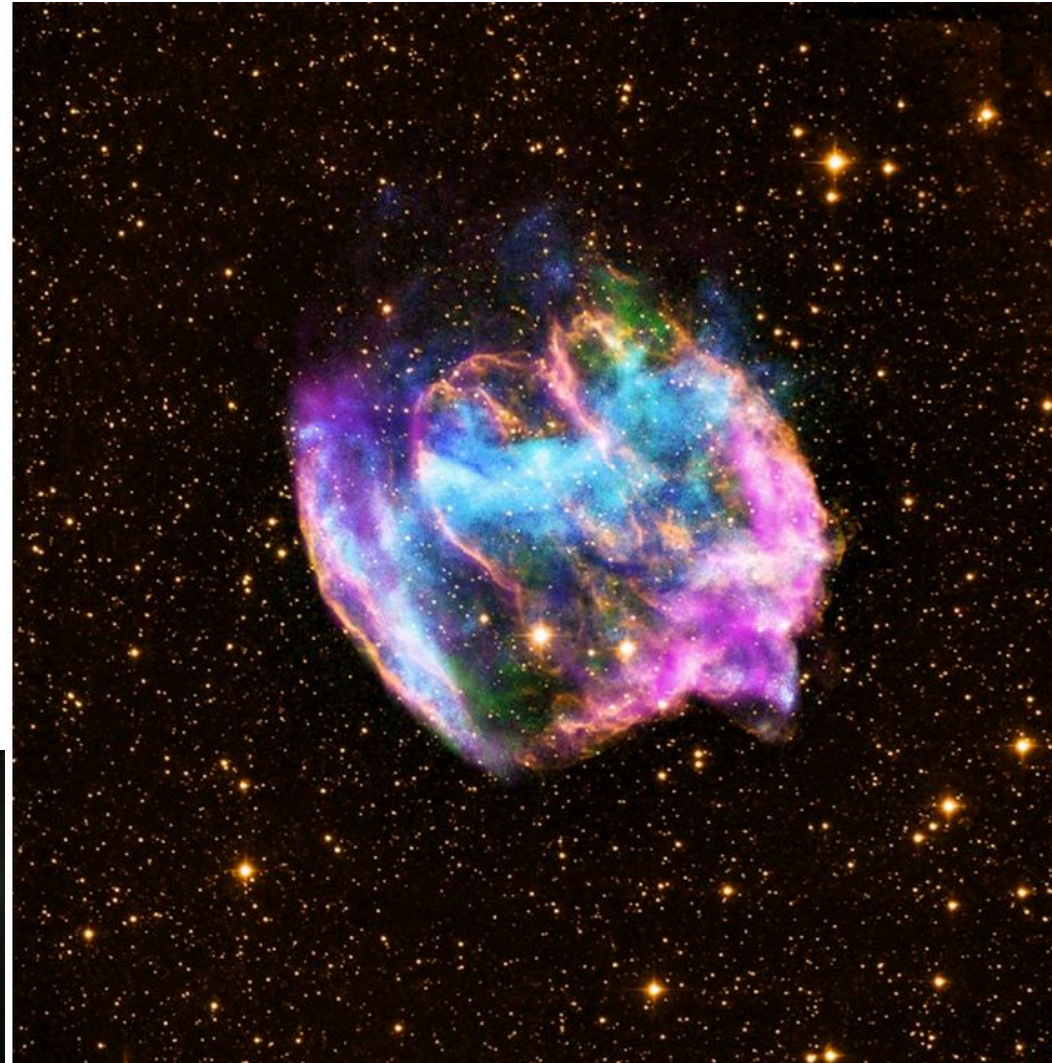
Stars-ISM

Stars affect the ISM through:

- UV radiation field
- Stellar wind
- Supernova explosion



Henry et al. 2002



Although most stellar explosions are fairly symmetrical, the supernova remnant W49B has an odd shape that could have resulted from the interaction of its magnetic field with its parent star.

(Image: © X-ray: NASA/CXC/MIT/L.Lopez et al; Infrared: Palomar; Radio: NSF/NRAO/VLA)

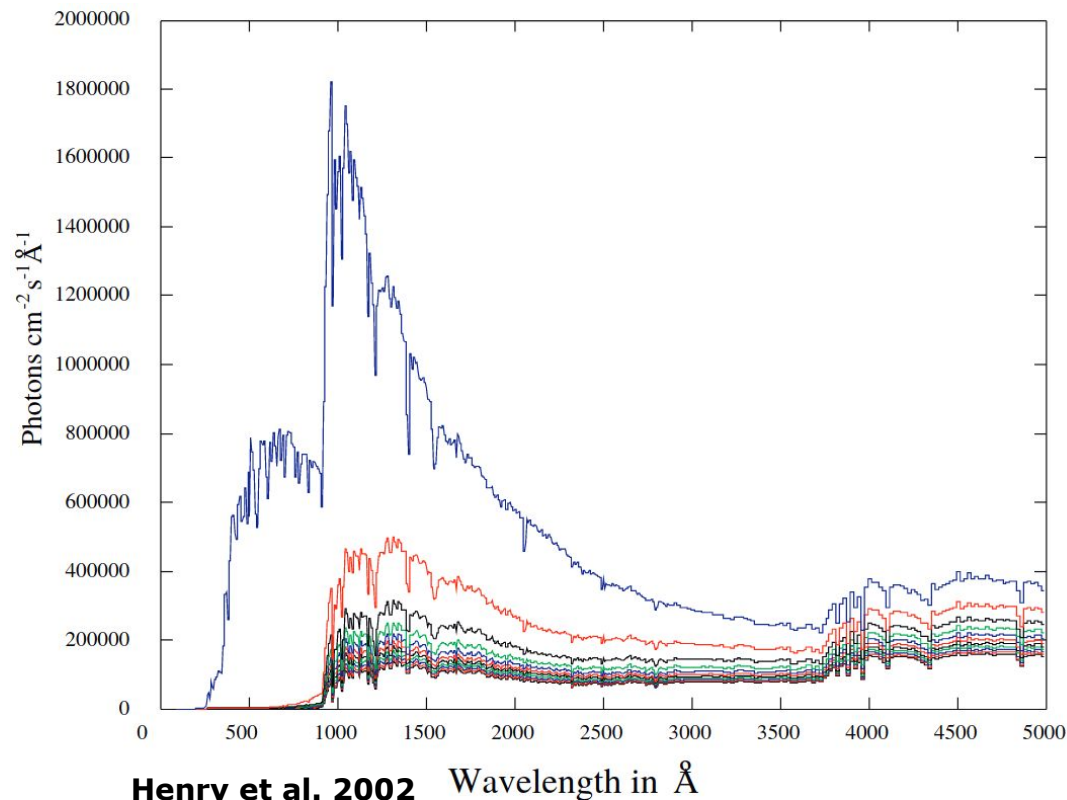


NGC 6240 as seen by the Hubble Space Telescope. Credit: NASA, ESA, the Hubble Heritage (STScI/AURA)-ESA/Hubble Collaboration, and A. Evans (University of Virginia, Charlottesville/NRAO/Stony Brook University)

UV radiation field

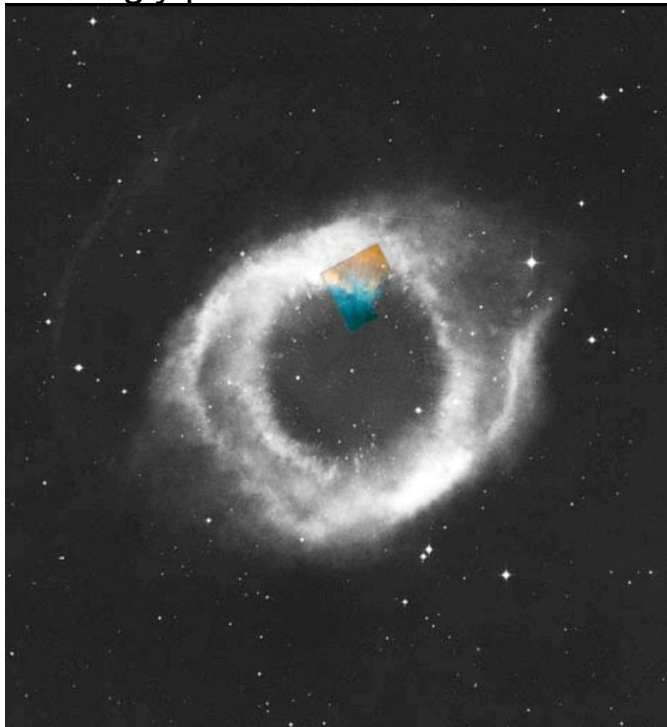
UV photons from O-B stars interacting with the ISM produce:

- 1) dissociation of H_2 molecules (if $\lambda < 1120 \text{ \AA}$) at the surface of molecular clouds (Federman et al., 1979), in photodissociation regions (Hollenbach and Tielens, 1999)
- 2) ionization of the gas: compact HII regions and more remote diffuse areas (warm ISM)
- 3) heat the ISM in the HII regions up to $\sim 8000 \text{ K}$, causing an expansion of the ionized bubble into the ambient ISM.

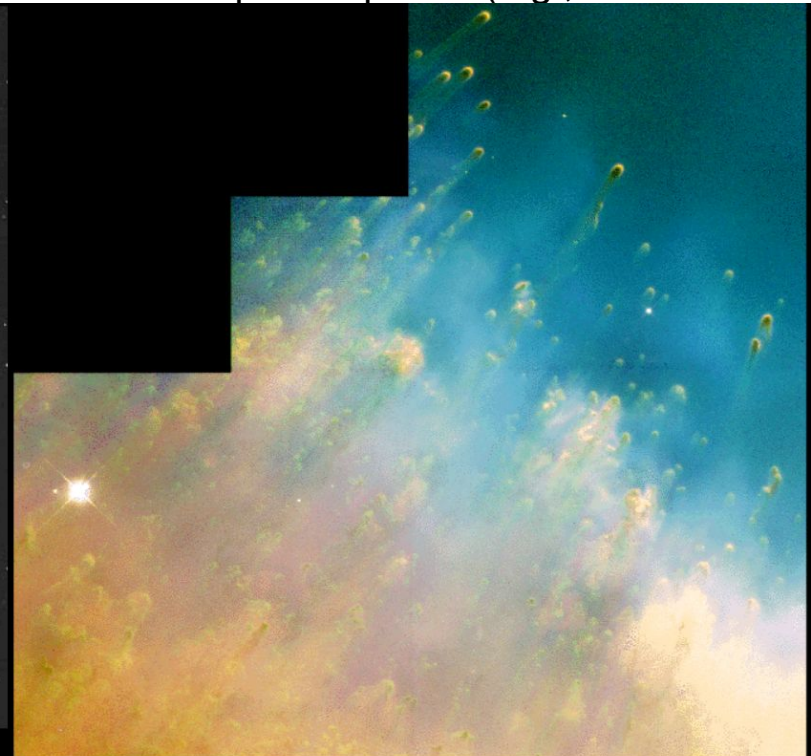


Stellar wind

- Low-mass stars before joining the main sequence (prolonged phase of hydrogen burning in the stellar core) experience energetic outflows (Lada, 1985).
- When stars go off the main sequence, they successively pass through the red-giant, asymptotic-giant-branch (AGB), and planetary-nebula stages, during which they lose mass (Salpeter, 1976; Knapp et al., 1990).
- High-mass stars suffer rapid mass loss throughout their lifetime (Conti, 1978; Bieging, 1990). Their wind becomes increasingly powerful over the course of the main-sequence phase (e.g., Schaller et al., 1992)



Helix Nebula • NGC 7293 • Las Campanas Observatory and HST
Black & White: J. Bedke (CSC/STScI), Carnegie Institution of Washington
Color Inset: C.R. O'Dell (Rice Univ.), NASA



Helix Nebula • NGC 7293

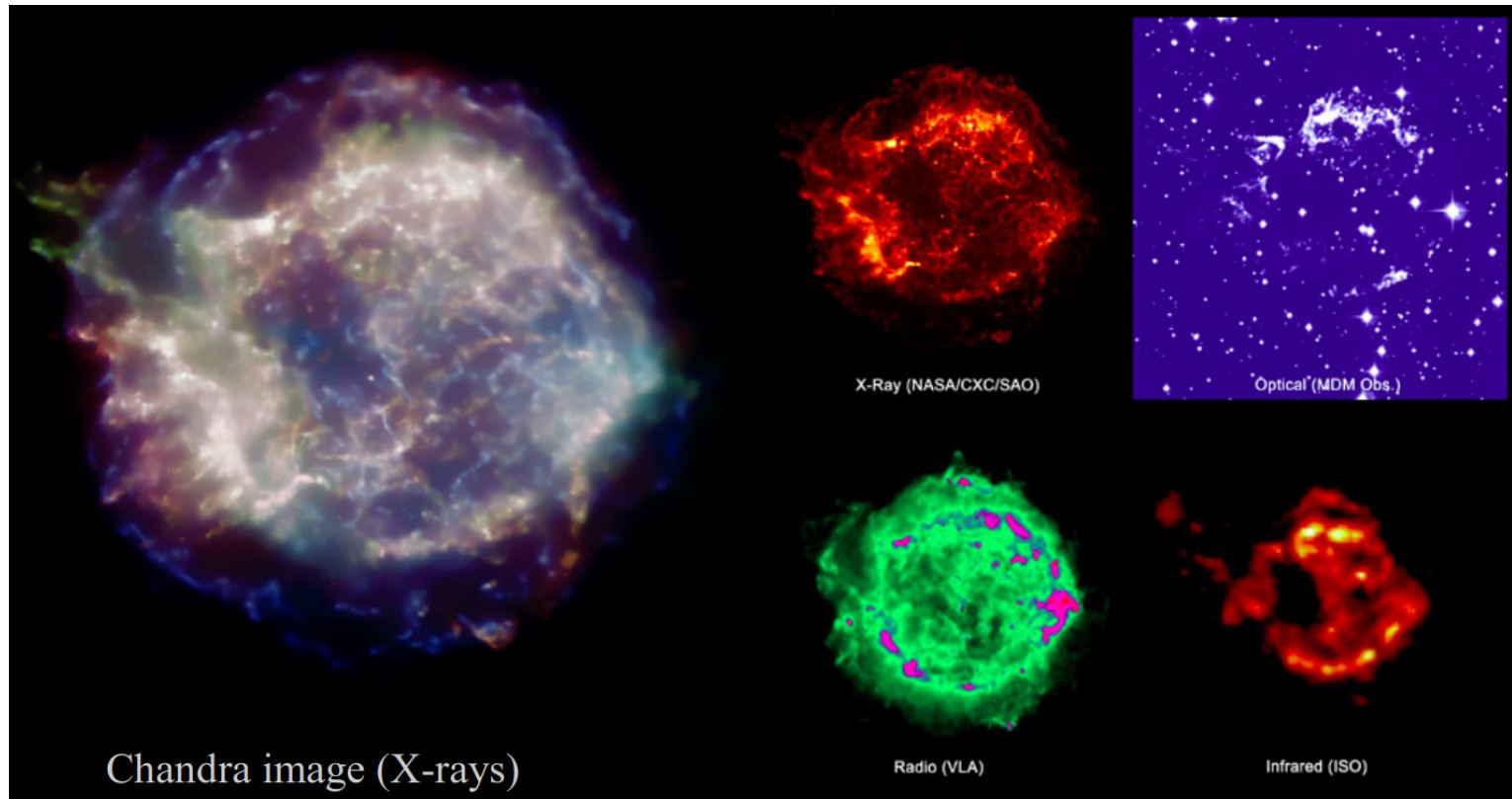
HST • WFPC2

PRC96-13a • ST ScI OPO • April 15, 1996 • C.R. O'Dell (Rice Univ.), NASA

Supernova explosion

Supernovae come into two types:

- Type I supernovae arise from old, low-mass stars, accreting material from a companion, which produces a thermonuclear instability.
- Type II supernovae arise from young stars with initial mass $> \sim 8M_{\odot}$, whose core collapses gravitationally once it has exhausted all its fuel (Woosley and Weaver, 1986).





What did we learn?

1. What is the ISM
2. Type of clouds
3. Molecular component of the ISM
4. Neutral component of the ISM
5. Dust component of the ISM
6. Stars-ISM relation